

Direct above-threshold ionization in intense few-cycle laser pulses: structures in the angle-integrated energy spectra

C. C. Chirilă

*Institute of High Performance Computing,
Agency for Science, Technology and Research,
1 Fusionopolis Way, #16-16 Connexis, Singapore 138632*

R. M. Potvliege

*Joint Quantum Centre (JQC) Durham-Newcastle,
Department of Physics, Durham University,
Durham DH1 3LE, United Kingdom*

Abstract

This paper concerns the theory of non-recollisional ionization or detachment of atoms or ions by intense few-cycle pulses. It is shown that in certain conditions of pulse duration, peak intensity and carrier-envelope phase, the ionization probability integrated over ejection angle varies almost periodically with energy, with a period roughly equal to the photon energy for slow enough outgoing electrons. This modulation is found both in calculations based on the strong field approximation (SFA) and in *ab initio* time-dependent calculations. It is explained as resulting from the interference between the contributions of different saddle times of the modified classical action. Methods for efficiently calculating the SFA ionization amplitude beyond the usual saddle point approximation are also discussed.

PACS numbers: 32.80.Rm,42.50.Hz

I. INTRODUCTION

Ever since the discovery of above-threshold ionization (ATI) [1], the energy spectrum of the electrons ejected from atoms or ions exposed to an intense laser pulse has proved rich in interesting features [2]. These include the suppression of the lowest ATI peaks in long pulses, which arises from the ponderomotive acceleration of the outgoing electron [3], prominent Stark-shift induced resonances in short pulses [4], the recollision plateau, which extends the spectrum well beyond the classical cutoff for direct ionization [5], and the low energy and very low energy structures recently found in ionization by ultrashort infrared pulses [6].

The theory of multiphoton ionization has progressed in parallel with these discoveries, through a combination of *ab initio* time-dependent calculations and of analyses based on the strong field approximation (SFA) or on the Floquet theory and other approaches [7]. Of particular note in the context of the present work is Keldysh's theory [8], a length-gauge formulation of the SFA which, since its inception fifty years ago, has been at the basis of a large fraction of the theoretical work on strong field physics. This formulation predicts accurate ionization probabilities for detachment from negative ions [9]. It is also both qualitatively and quantitatively correct for ionization from atoms, provided the Coulomb interaction between the active electron and the residual ion is properly taken into account [10].

In this article we study another feature of ionization in intense ultra-short laser pulses, namely an almost periodic modulation marking the angle-integrated energy spectrum in appropriate conditions of pulse duration, peak intensity and carrier-envelope phase. Although this modulation is readily found both in SFA calculations and in *ab initio* calculations, we are not aware that it has been discussed previously [11]. However, like various other strong field phenomena, it can be traced, through the SFA, to the interplay between different saddle times of the modified classical action. We concentrate on the low energy end of the ionization spectrum, where this modulation is clearest. As is well known, this part of the spectrum is dominated by direction ionization. Recollision of the detached electron with the residual ion plays no role here, and is therefore neglected in our analysis.

The theoretical background to the work is outlined in Section II. The results are presented and discussed in Section III. Technical issues concerning the calculation of the ionization

amplitude within the SFA are briefly considered in the Appendix — namely avoiding the spurious contributions made to the ionization amplitude by the end points of the integral defining it, computational methods bypassing saddle point integration, and improving the accuracy of the usual (second order) saddle point method. Atomic units are assumed throughout this article, except where specified otherwise.

II. THEORY

We work within the dipole approximation and describe the laser pulse by a spatially homogeneous vector potential $\mathbf{A}(t)$ and a spatially homogeneous electric field $\mathbf{F}(t) = -\partial_t \mathbf{A}(t)$. Specifically, we set

$$\mathbf{A}(t) = (F_0/\omega)\chi(t)\hat{\mathbf{e}}\sin(\omega t + \varphi), \quad (1)$$

where $\hat{\mathbf{e}}$ is a unit vector (we assume linear polarization), $\chi(t)$ is a function defining the pulse's intensity profile, and φ is an arbitrary phase [12]. We assume that $\chi(t)$ peaks at $t = 0$. Most of the results presented below are calculated for pulses with a half-period \cos^2 amplitude envelope encompassing an integer number of optical cycles, for which

$$\chi(t) = \begin{cases} \cos^2\left(\frac{\omega t}{2n_c}\right) & -n_c\pi/\omega \leq t \leq n_c\pi/\omega \\ 0 & t < -n_c\pi/\omega \quad \text{or} \quad t > n_c\pi/\omega, \end{cases} \quad (2)$$

where n_c is the number of optical cycles encompassed by the pulse. Such pulses have the desirable property of not imparting an unphysical displacement or drift momentum to a free electron [13]. We also consider pulses with a sech amplitude profile (sech^2 in intensity). In either case, both $|\mathbf{A}(t)|$ and $|\mathbf{F}(t)|$ are negligibly small, if not exactly zero, before a certain time t_i and after a certain time t_f .

For simplicity, we assume that the atom has only one active electron and is initially in a certain bound state with wave function $\Phi_0(\mathbf{r}, t) = \phi_0(\mathbf{r}) \exp(I_p t)$. In Keldysh's formulation of the strong field approximation, the probability amplitude for the photoelectron to have a momentum \mathbf{p} at times $t \geq t_f$ is then

$$A_{\mathbf{p}0}^{(K)} = -i \int_{t_i}^{t_f} dt \int d\mathbf{r} \Psi_{\mathbf{p}}^*(\mathbf{r}, t) [\mathbf{r} \cdot \mathbf{F}(t)] \Phi_0(\mathbf{r}, t), \quad (3)$$

within an irrelevant phase factor. The wave function $\Psi_{\mathbf{p}}(\mathbf{r}, t)$ is the Volkov wave

$$\Psi_{\mathbf{p}}(\mathbf{r}, t) = \frac{1}{(2\pi)^{3/2}} \exp \left[i\boldsymbol{\pi}(\mathbf{p}, t) \cdot \mathbf{r} - \frac{i}{2} \int_{t_i}^t dt' \boldsymbol{\pi}^2(\mathbf{p}, t') \right], \quad (4)$$

where $\boldsymbol{\pi}(\mathbf{p}, t)$ denotes the kinematical momentum of the electron:

$$\boldsymbol{\pi}(\mathbf{p}, t) = \mathbf{p} + \mathbf{A}(t). \quad (5)$$

In this formulation, the interaction between the photoelectron and the ionic core is treated exactly in the initial state of the system but is otherwise completely neglected. As is well known, the effect of this long range interaction on the motion of the electron during the tunnelling stage of the ionization process can be taken into account semiclassically, and doing so brings the predictions of the theory into much closer agreement with experiment. For a stationary laser field of electric field amplitude F_0 , the correction amounts to multiplying $\Psi_{\mathbf{p}}(\mathbf{r}, t)$ by the factor [14]

$$I(r) = \left(\frac{4I_p}{F_0} \frac{1}{r} \right)^{Z/\kappa}, \quad (6)$$

where Z is the charge of the residual ion and $\kappa = (2I_p)^{1/2}$. Although derived for a stationary field, this correction, with F_0 taken to the peak electric field amplitude, has been shown to be effective for ultra short laser pulses [10]. Rather than the Keldysh amplitude (3), we thus work with the ‘‘tunnelling corrected’’ amplitude

$$A_{\mathbf{p}0} = -i \int_{t_i}^{t_f} dt \int d\mathbf{r} \Psi_{\mathbf{p}}^*(\mathbf{r}, t) I(r) [\mathbf{r} \cdot \mathbf{F}(t)] \Phi_0(\mathbf{r}, t). \quad (7)$$

Given the normalization of the Volkov wave (4), the density of probability that an electron is detached by the pulse with a final kinetic energy $E = p^2/2$ is

$$P(E) = 2\pi \int_0^\pi P(E, \theta) \sin \theta d\theta, \quad (8)$$

with θ the angle between the momentum \mathbf{p} and the polarization vector $\hat{\mathbf{e}}$ and

$$P(E, \theta) = p |A_{\mathbf{p}0}|^2. \quad (9)$$

Eq. (7) can also be written in the form

$$A_{\mathbf{p}0} = -\frac{1}{(2\pi)^{3/2}} \int_{t_i}^{t_f} dt \int d\mathbf{r} \left(\frac{\partial}{\partial t} \exp[-i\boldsymbol{\pi}(\mathbf{p}, t) \cdot \mathbf{r}] \right) I(r) \phi_0(\mathbf{r}) \exp[iS(\mathbf{p}, t)], \quad (10)$$

with

$$S(\mathbf{p}, t) = \frac{1}{2} \int_{t_i}^t \boldsymbol{\pi}(\mathbf{p}, t')^2 dt' + I_p t. \quad (11)$$

Upon integrating by parts, we thus have

$$A_{\mathbf{p}0} = -\frac{1}{(2\pi)^{3/2}} \exp[iS(\mathbf{p}, t)] M_{\mathbf{p}0}(t) \Big|_{t_i}^{t_f} + \frac{i}{(2\pi)^{3/2}} \int_{t_i}^{t_f} \exp[iS(\mathbf{p}, t)] S'(\mathbf{p}, t) M_{\mathbf{p}0}(t) dt \quad (12)$$

where $S'(\mathbf{p}, t)$ is the derivative of $S(\mathbf{p}, t)$ with respect to time and

$$M_{\mathbf{p}0}(t) = \int \exp[-i\boldsymbol{\pi}(\mathbf{p}, t) \cdot \mathbf{r}] I(r) \phi_0(\mathbf{r}) d\mathbf{r}. \quad (13)$$

As we will soon see, the boundary terms appearing in Eq. (12) are exactly cancelled by opposite contributions from the end-points of the integral. We note from Eq. (7) that in fact the ionization amplitude $A_{\mathbf{p}0}$ does not depend on the precise values of the initial and final times t_i and t_f , as long as the pulse's electric field is effectively zero at and around t_i and at t_f (as should be expected on physical grounds — the ionization probability cannot depend on how the field varies at times where it is too weak to affect the atom). Mathematically, there is no dependence on t_i and t_f only if $\mathbf{E}(t)$ and all the derivatives of $\mathbf{E}(t)$ vanish at these two times [15]. This condition is not met by the model of pulses commonly used in calculations, which might have practical consequences if pulses with an excessively fast turn on and turn off are considered (this issue is considered further in the Appendix but is normally not problematic in applications to realistic cases).

More specifically, we represent the initial state of the atom by an s-orbital and, following [16], set

$$\phi_0(\mathbf{r}) \equiv 2\kappa^{3/2} C_{\kappa 0} (\kappa r)^{(Z/\kappa)-1} \exp(-\kappa r) / \sqrt{4\pi}, \quad (14)$$

where $C_{\kappa 0}$ is the asymptotic coefficient for the species considered in the definition of [17]. Accordingly, the product $S'(\mathbf{p}, t)M_{\mathbf{p}0}(t)$ reduces to $(4\pi\kappa)^{1/2}(4I_p\kappa/F_0)^{Z/\kappa}C_{\kappa 0}$, and [18]

$$A_{\mathbf{p}0} = i \frac{(2\kappa)^{1/2} C_{\kappa 0}}{2\pi} \left(\frac{4I_p\kappa}{F_0} \right)^{Z/\kappa} \left(\int_{t_i}^{t_f} \exp[iS(\mathbf{p}, t)] dt - \frac{\exp[iS(\mathbf{p}, t)]}{iS'(\mathbf{p}, t)} \Big|_{t_i}^{t_f} \right). \quad (15)$$

In this article we present results for detachment from the ground state of an He^+ ion or an hydrogen atom, for which $C_{\kappa 0} = 1$, and for ionization from the ground state of neutral helium, for which it is appropriate to take $C_{\kappa 0} = 0.993$ [17].

The integral appearing in the right-hand side of Eq. (15) is amenable to saddle point integration, which is the usual way of calculating the ionization amplitude in the strong field approximation. Within this approach,

$$\int_{t_i}^{t_f} \exp[iS(\mathbf{p}, t)] dt \approx \sum_j \sqrt{\frac{2\pi i}{S''(\mathbf{p}, t_j)}} \exp[iS(\mathbf{p}, t_j)] + \frac{\exp[iS(\mathbf{p}, t)]}{iS'(\mathbf{p}, t)} \Big|_{t_i}^{t_f} + \dots \quad (16)$$

where the times t_j are the complex values of t at which $S'(\mathbf{p}, t) = 0$. The first term in the right-hand side of Eq. (16) is the contribution to the integral of the saddle times t_j , while

the second term is the dominant contribution of the end-points t_i and t_f of the integration contour (dominant in the sense of an asymptotic analysis, see, e.g., [19]). Depending on the pulse, the second term can be large, even much larger than the first term; however, as shown by Eq. (15), it is exactly cancelled by the boundary terms arising from the integration by parts. The remainder, not written down explicitly in the equation, is the sum of the higher-order contributions of these two end-points and of the saddle times. Since the choice of t_i and t_f is arbitrary, it is appropriate to neglect the end-point contributions altogether and write

$$A_{\mathbf{p}0} \approx i \frac{(2\kappa)^{1/2} C_{\kappa 0}}{2\pi} \left(\frac{4I_p \kappa}{F_0} \right)^{Z/\kappa} \sum_{t_j} \sqrt{\frac{2\pi i}{S''(\mathbf{p}, t_j)}} \exp[iS(\mathbf{p}, t_j)]. \quad (17)$$

However, for maximum accuracy, we prefer not to use the saddle point method to calculate the energy spectrum. Instead, we treat time as a complex variable and numerically integrate the function $\exp[iS(\mathbf{p}, t)]$ over t along a straight line path parallel to the real axis and passing through the saddle point with the lowest positive imaginary part. This approach and other alternative methods for integrating this function over the duration of the pulse are discussed in the Appendix.

III. RESULTS AND DISCUSSION

As is well known, the ionization probability predicted by the SFA is generally an oscillating function of the detachment energy E and of the angle of emission θ , due to interferences between the contributions of different saddle times t_j . Examples of this oscillatory behavior are shown in Fig. 1 for the case of a strong 800 nm 4-cycle pulse interacting with an He^+ ion. Panel (a) illustrates the variation of $P(E, \theta)$ for a “cosine-like” pulse ($\varphi = 0$), panel (b) for a “sine-like” pulse ($\varphi = \pi/2$). Comparing these two sets of results, it can be seen that the energies at which $P(E, \theta)$ is maximal tend to vary less with the emission angle for $\varphi = 0$ than for $\varphi = \pi/2$. In particular, for $\varphi = 0$ the peaks tend to come in groups concentrated in the same ranges of energies for all values of θ .

This feature is more striking in the angle-integrated spectra shown in Fig. 2: the propensity of $P(E, \theta)$ to be largest in the same ranges of values of E (almost) irrespective of θ results in broad, almost regularly spaced peaks modulating the angle-integrated probability $P(E)$ when $\varphi \approx 0$. For the pulse duration and intensity considered in Fig. 2, these peaks

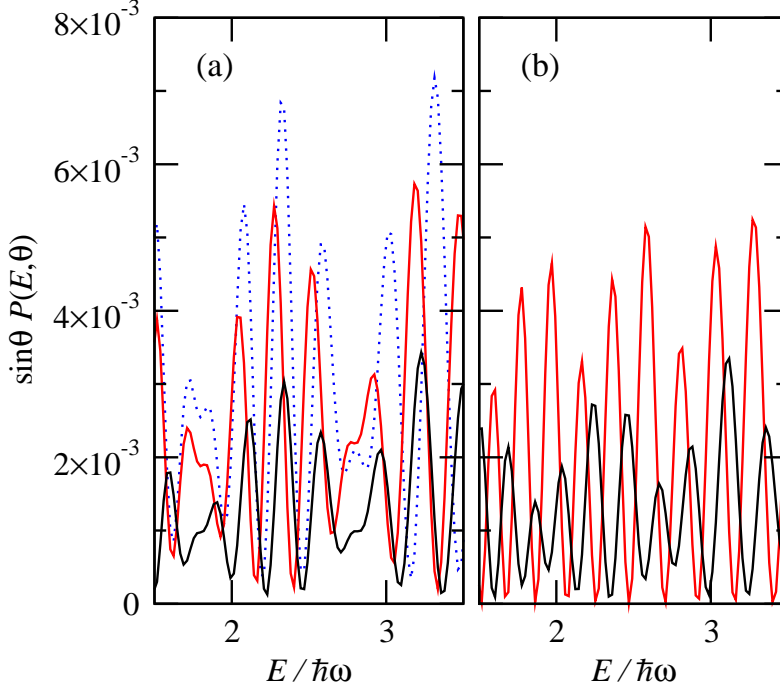


FIG. 1: (Color online) The probability of detachment from the ground state of He^+ by a 4-cycle \cos^2 pulse, (a) for $\varphi = 0$, (b) for $\varphi = \pi/2$. The carrier wavelength is 800 nm and the peak intensity is about $5.6 \times 10^{15} \text{ W cm}^{-2}$ ($F_0 = 0.4$ a.u. exactly). Solid black curves: $\theta = \pi/20$. Solid red curves: $\theta = \pi/10$. Dotted blue curve (left panel only): $\theta = 3\pi/20$.

rapidly decrease in contrast when φ increases and they do not manifest for $\varphi = \pi/2$. The peaks found for $\varphi \approx 0$, which are almost regularly spaced by the photon energy, are reminiscent of the well-known ATI peaks observed in long-pulse experiments [7]. However, their origin is different. Here ponderomotive scattering plays no role and, as discussed below, these structures arise directly from the way the modified classical action $S(\mathbf{p}, t)$ varies with the angle of emission. The spacing between the peaks found for few-cycle pulses is actually energy-dependent, although this feature is not visible in Fig. 2

That these structures are not an artefact of the strong field approximation is shown by Fig. 3, for a 400 nm pulse: the angle-integrated spectra obtained by solving the time-dependent Schrödinger equation *ab initio* are very similar to the SFA spectra and have the same periodic structure, apart for an unimportant difference in overall amplitude and a shift in the position of the peaks [20]. A shift due to the Coulomb interaction between the outgoing electron and the parent ion can be expected — see, e.g., [10]. However, the predictions of the strong field approximation are well verified by the *ab initio* calculation. (Also shown in Fig. 3, and

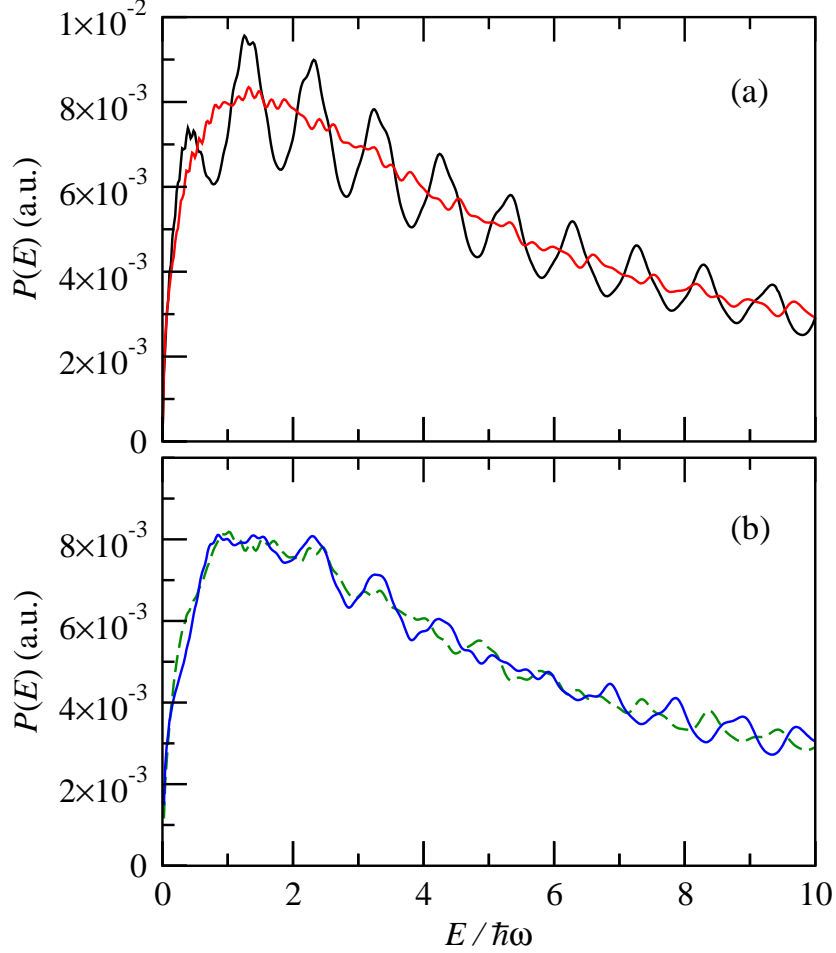


FIG. 2: (Color online) The angle-integrated probability of detachment from the ground state of He^+ by a 4-cycle \cos^2 pulse, (a) for $\varphi = 0$ (black curve) or $\varphi = \pi/2$ (red curve), (b) for $\varphi = \pi/10$ (blue solid curve) or $\varphi = \pi/5$ (green dashed curve). As in Fig. 1, the carrier wavelength is 800 nm and $F_0 = 0.4$ a.u. (about 5.6×10^{15} W cm^{-2} peak intensity).

represented by a dashed curve, is the spectrum obtained by projecting the time-dependent wave function onto plane waves, at the end of the pulse, after this time-dependent wave function has been orthogonalized to the initial state. This approximate spectrum is a better comparison and is in better agreement with the SFA spectrum since it is not affected by the Coulomb force acting on the outgoing electron after the end of the pulse.)

However, observing these structures in a high-intensity experiment is likely to be problematic, as the spectrum depends sensitively on the parameters of the pulse. For example, the results of Fig. 4 show that a mere 1% change in the peak intensity, from 1.00 to 1.01×10^{15} W cm^{-2} , shifts the peaks very significantly in the case of helium atoms ionized by a few-cycle

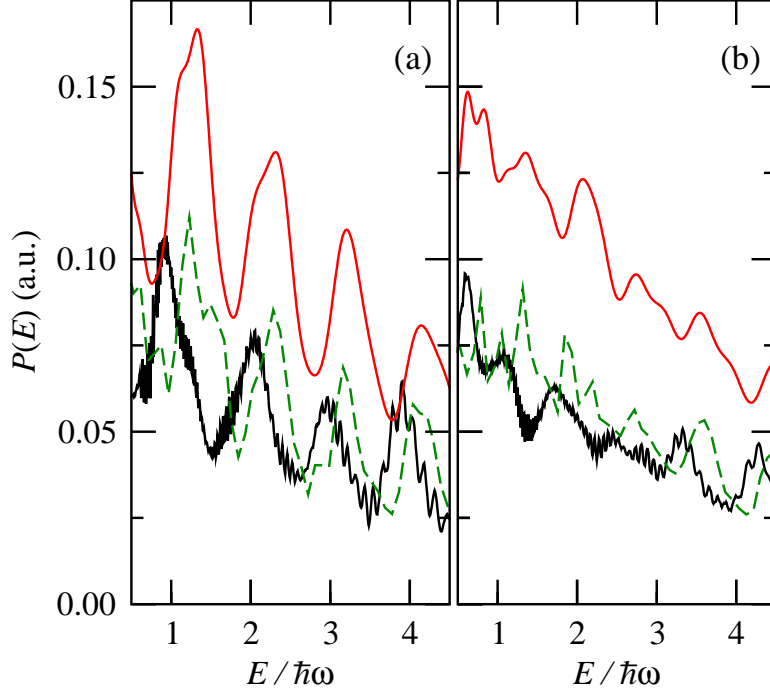


FIG. 3: (Color online) The angle-integrated probability of detachment from the ground state of He^+ by a \cos^2 pulse encompassing exactly 4 optical cycles. Here the carrier wavelength is 400 nm and the peak intensity of the pulse is $1 \times 10^{16} \text{ W cm}^{-2}$. (a): $\varphi = 0$. (b): $\varphi = \pi/2$. Solid black curves: Spectrum obtained by solving the time-dependent Schrödinger equation *ab initio*. Solid red curves: Predictions of the strong field approximation. Dashed green curves: The same as the solid black curves, but with the spectrum calculated by projecting the wave function on plane waves.

800 nm pulse. (The amplitude envelope was taken to be a sech function in these calculations, rather than a \cos^2 function.) Clearly, in experiments using such strong fields, the peaks and troughs structure of the energy spectrum would be averaged out by the unavoidable spatial variation of the pulses' intensity profile over the interaction region.

The origin of these peaks can be understood by analyzing how the ionization probability depends on the interference between the contribution of the different saddle times, in the approximation where the ionization amplitude is given by Eq. (17). In this approximation,

$$P(E, \theta) \approx pC \left(\sum_{j=1}^{n_s} I_{jj} + 2 \sum_{j=1}^{n_s-1} \sum_{k=j+1}^{n_s} I_{jk} \right), \quad (18)$$

where n_s is the number of saddle times making a non-negligible contribution to $P(E, \theta)$, C

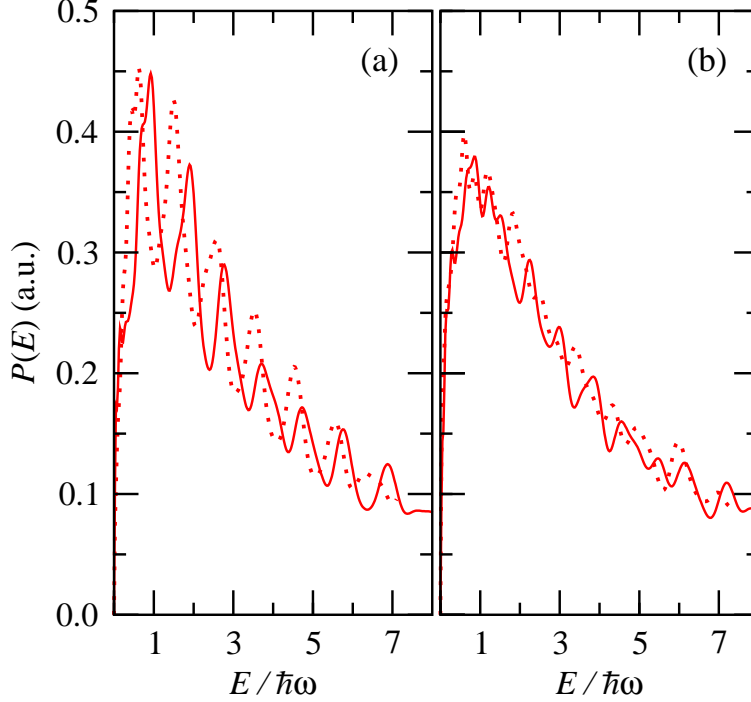


FIG. 4: (Color online) The probability of detachment from the ground state of neutral helium by a few-cycle pulse. The carrier wavelength is 800 nm. The pulse has a sech-profile in amplitude with a full width at half maximum of 2 optical cycles. The peak intensity is either $1.00 \times 10^{15} \text{ W cm}^{-2}$ (solid curves) or $1.01 \times 10^{15} \text{ W cm}^{-2}$ (dotted curves). (a): $\varphi = 0$. (b): $\varphi = \pi/2$.

is a real positive constant, and

$$I_{jk} = 2\pi \text{Re} \left([S''(\mathbf{p}, t_j) S''^*(\mathbf{p}, t_k)]^{-1/2} \exp[iS(\mathbf{p}, t_j) - iS^*(\mathbf{p}, t_k)] \right). \quad (19)$$

it is worth noting that I_{jk} would be exactly proportional to $\cos[\text{Re} S(\mathbf{p}, t_j) - \text{Re} S(\mathbf{p}, t_k)]$ if $S''(\mathbf{p}, t_j)$ and $S''^*(\mathbf{p}, t_k)$ had no imaginary part. The terms in I_{jk} with $k \neq j$ may thus vary rapidly with E and θ while those with $k = j$ normally vary slowly.

In view of Eqs. (1), (5) and (11), the saddle times t_j and t_k are solutions of the equation

$$(F_0/\omega)\chi(t) \sin(\omega t + \varphi) = -p_{\parallel} \pm i\sqrt{2I_p + p_{\perp}^2}, \quad (20)$$

where $p_{\parallel} = p \cos \theta$ and $p_{\perp} = p \sin \theta$. (Only those solutions of this equation that have a positive imaginary part are relevant in this context.) For the small values of E we are considering here, the complex values of t obtained by solving Eq. (20) are sufficiently close to the real values of t at which $\mathbf{A}(t) = 0$ that each relevant solutions can be sought by expanding $\mathbf{A}(t)$ in powers of the difference $(t - t_0)$, where t_0 is the zero of $\mathbf{A}(t)$ closest to the

saddle time considered. Doing so and limiting oneself to terms of second order in $(t - t_0)$ yields

$$\begin{aligned} \text{Re } S(\mathbf{p}, t_j) - \text{Re } S(\mathbf{p}, t_k) \approx & \\ & (E + I_p)(t_{0j} - t_{0k}) + \frac{1}{2} \int_{t_{0j}}^{t_{0k}} A^2(t) dt + a_{jk} p_{\parallel} \\ & + p_{\parallel} \left(I_p + \frac{p^2 + 2p_{\perp}^2}{6} \right) \left[\frac{1}{E(t_{0k})} - \frac{1}{E(t_{0j})} \right], \end{aligned} \quad (21)$$

where t_{0j} and t_{0k} are the real solutions of the equation $\mathbf{A}(t) = 0$ closest to the complex saddle times t_j and t_k and

$$a_{jk} = \int_{t_{0j}}^{t_{0k}} \hat{\mathbf{e}} \cdot \mathbf{A}(t) dt. \quad (22)$$

We stress that Eq. (21) applies only for low momenta of the ejected electron, which is the part of the spectrum we focus on in this work.

The difference $\text{Re } S(\mathbf{p}, t_j) - \text{Re } S(\mathbf{p}, t_k)$ thus depends on the angle of ejection θ primarily through a term proportional to the integral a_{jk} and a term proportional to the difference $1/E(t_{0k}) - 1/E(t_{0j})$. Hence, the contribution to $P(E, \theta)$ of those pairs of saddle times for which $a_{jk} \approx 0$ together with $E(t_{0j}) \approx E(t_{0k})$ varies little with the ejection angle θ .

In the definition of the pulse adopted in this work, where the pulse envelope is symmetric and peaks at $t = 0$, such pairs of saddles exist for $\varphi = 0$: for this carrier-envelope phase, $\mathbf{A}(t) = 0$ at $t_{01} = -\pi/\omega$, $t_{02} = 0$ and $t_{03} = \pi/\omega$, besides other values of t of lesser relevance for a few-cycle pulse (because the corresponding electric field is somewhat weaker than at t_{01} , t_{02} and t_{03}). Let us call t_1 , t_2 and t_3 the complex saddle times closest to, respectively, t_{01} , t_{02} and t_{03} . The contribution of t_1 and t_3 to $P(E, \theta)$ is (almost) angle-independent since $a_{13} = 0$ and $E(t_{01}) = E(t_{03})$. The interference between these two saddle times is constructive rather than destructive, giving a peak in the spectrum, at the values of E for which $E \approx E_N$, where

$$E_N = N\omega - \left[I_p + \frac{\omega}{4\pi} \int_{-\pi/\omega}^{\pi/\omega} A^2(t) dt \right] \quad (23)$$

with N an integer [21]. The angular distribution will also depend on interferences between the contributions of t_2 and either t_1 or t_3 . However, since the corresponding values of a_{jk} and $1/E(t_{0k}) - 1/E(t_{0j})$ are non-zero, these contributions oscillate rapidly with θ and hardly manifest in the angle-integrated spectrum.

Turning to the case of $\varphi \approx \pi/2$, the most relevant saddle times for few-cycle pulses are $t_1 \approx t_{01} \equiv -3\pi/2\omega$, $t_2 \approx t_{02} \equiv -\pi/2\omega$, $t_3 \approx t_{03} \equiv \pi/2\omega$ and $t_4 \approx t_{04} \equiv 3\pi/2\omega$. For the peak

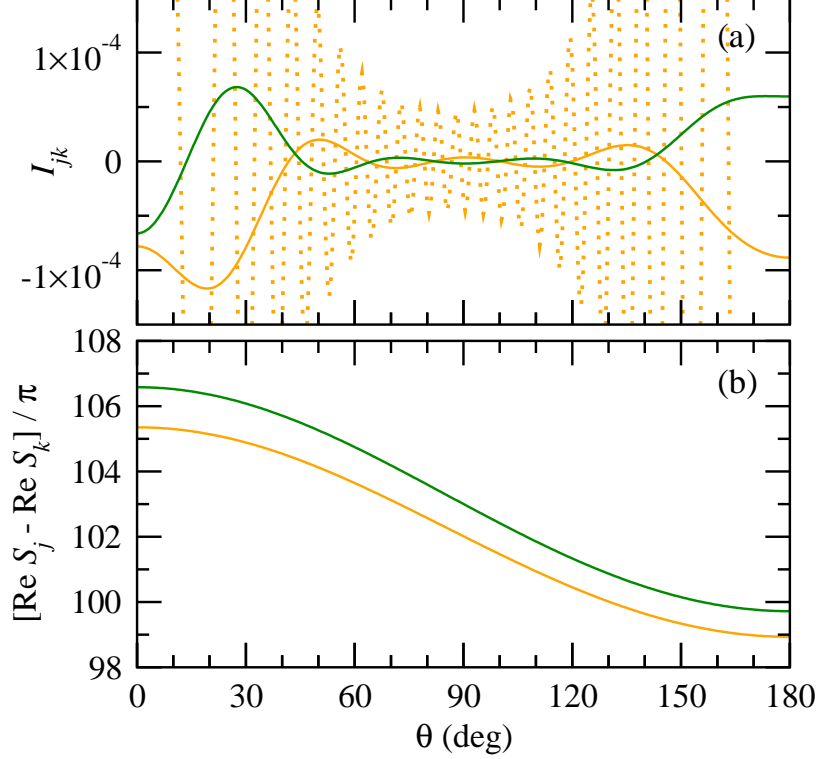


FIG. 5: (Color online) Contribution of individual saddle times to the ionization amplitude for the same system as in Fig. 4(b), either for $E = 3.4 \hbar\omega$ (light orange curves) or $E = 3.9 \hbar\omega$ (dark green curves) (the pulse peak intensity is $1 \times 10^{15} \text{ W cm}^{-2}$). (a): Difference between the real part of the modified classical action at two different saddle times, divided by π . (b): The quantity I_{jk} defined by Eq. (19). Solid curves: $t_j \approx -3\pi/2\omega$ and $t_k \approx \pi/2\omega$. Dotted curve: $t_j \approx -\pi/2\omega$ and $t_k \approx \pi/2\omega$.

intensity and pulse duration of Fig. 2, however, the electric field is too weak at t_1 and t_4 for these saddle times to play an important role, and only t_2 and t_3 need to be considered. Since $a_{23} \neq 0$ and $E(t_{02}) \neq E(t_{03})$, $P(E, \theta)$ oscillates rapidly both as a function of E and of θ , and the resulting angle-integrated spectrum is almost structureless [Fig. 2(a)].

Other saddle times can become significant in longer pulses or closer to saturation. For example, the peaks and troughs visible in Figs. 3 and 4 in the angle-integrated angular distribution for $\varphi = \pi/2$ arise from contributions from the saddle times t_1 and t_4 defined in the previous paragraph, besides t_2 and t_3 . The structures found in the case of Fig. 4(b) are analyzed in Fig. 5. Part (a) of the latter shows how I_{13} and I_{23} vary with the ejection angle θ at either $E = 3.4 \hbar\omega$ (where the angle-integrated spectrum has a peak) or $3.9 \hbar\omega$ (the adjacent trough). I_{13} , represented by the solid curves, oscillates much less than I_{23} (the

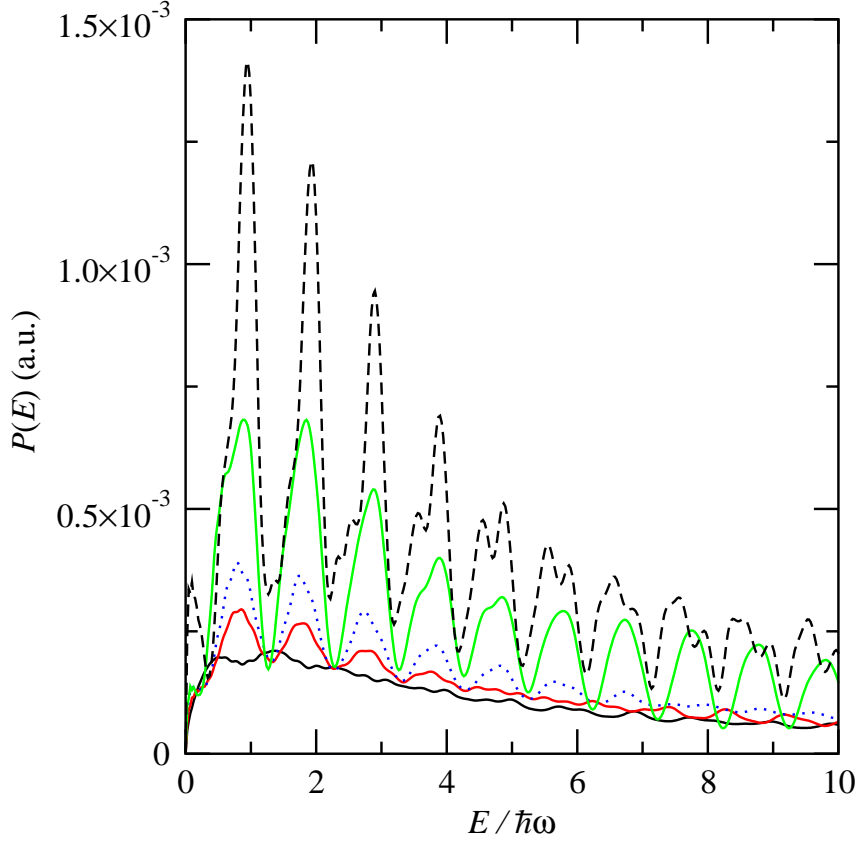


FIG. 6: (Color online) The angle-integrated probability of detachment from the ground state of He^+ by a \cos^2 pulse encompassing exactly n_c optical cycles. As in Figs. 1 and 2 the carrier wavelength is 800 nm; however here $F_0 = 0.3$ a.u., corresponding to a peak intensity of about 3.2×10^{15} W cm^{-2} , and $\varphi = 0.23$. Solid black curve: $n_c = 4$. Solid red curve: $n_c = 5$. Dotted blue curve: $n_c = 6$. Solid green curve: $n_c = 10$. Dashed black curve: $n_c = 15$.

dotted curve) both because $|a_{13}| \ll |a_{23}|$ and because $E(t_1) \approx E(t_3)$ whereas $E(t_2) = -E(t_3)$ (a_{13} and $E(t_1) - E(t_3)$ would be zero if the field had a constant intensity). As seen from the figure, I_{13} keeps the same sign in the angular regions where this term contributes most to the ionization probability [22]. Positive values give a peak in the angle integrated spectrum, and negative values a trough. Increasing E leads to a near-periodic succession of peaks and troughs because, as seen from Fig. 5(b), $\text{Re}[S(\mathbf{p}, t_1) - S(\mathbf{p}, t_3)]$ increases almost uniformly with E . I_{13} oscillates between positive and negative values as $\text{Re}[S(\mathbf{p}, t_1) - S(\mathbf{p}, t_3)]$ sweeps through half integer multiples of π (or thereabout).

Increasing the pulse duration increases the number of saddle times contributing significantly to the ionization probability. The impact of this change on the structure of the

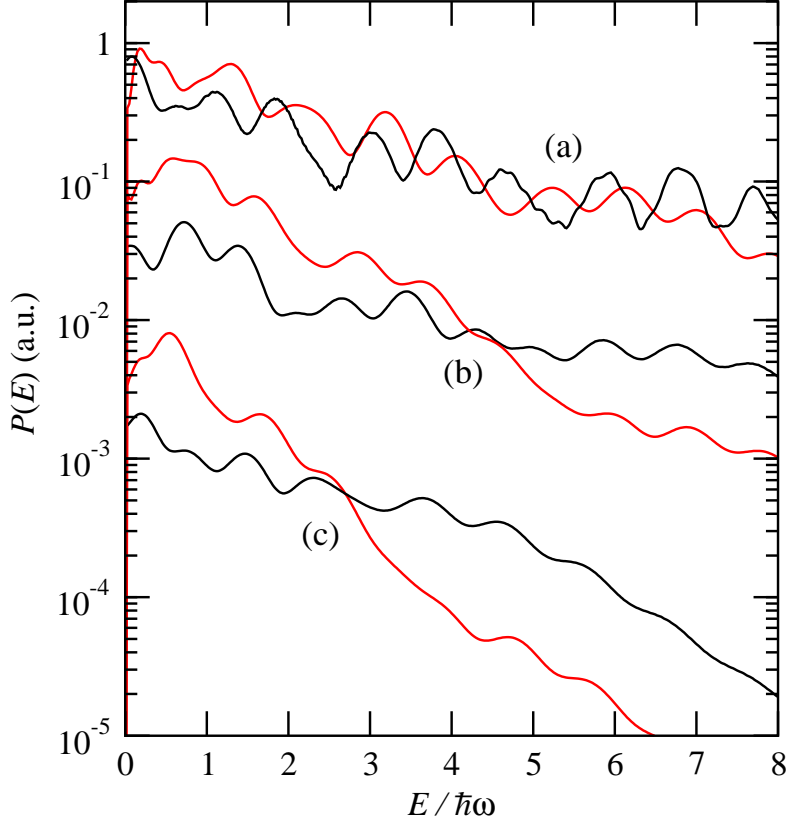


FIG. 7: (Color online) The angle-integrated probability of ionization from the ground state of atomic hydrogen by a \cos^2 pulse encompassing exactly 4 optical cycles. The carrier wavelength is 800 nm and $\varphi = 0$. The peak intensity of the pulse is (a) 2×10^{14} W cm $^{-2}$, (b) 1×10^{14} W cm $^{-2}$ or (c) 5×10^{13} W cm $^{-2}$. Black curves: Spectrum obtained by solving the time-dependent Schrödinger equation *ab initio*. Red curves: Predictions of the strong field approximation.

angle-integrated energy spectrum is illustrated by Fig. 6. The results shown in this figure were calculated for the same system as in Fig. 2 but for a smaller intensity and for a single value of the carrier-envelope phase ($\varphi = 0.23$ in Fig. 6). At the intensity considered, ionization occurs almost entirely in the vicinity of the maximum of the pulse envelope. As only one saddle time is important, that closest to $t = 0$, the spectrum is almost structureless. The other saddle times become more significant for longer pulse durations. As a result, the peaks are more contrasted for 5-cycle pulses, very obvious for 6- and, particularly, 10-cycle pulses, and then tend to split into subpeaks for still longer pulses.

Interestingly, the structures discussed above seem to subsist down to much lower intensities. Both *ab initio* and SFA calculations in atomic hydrogen for 4-cycle 800 nm pulses yield

angle-integrated energy spectra modulated by near-periodic maxima separated by about $\hbar\omega$, down to intensities as low as $5 \times 10^{13} \text{ W cm}^{-2}$ (Fig. 7). Although here the SFA results are not as close in agreement with the *ab initio* results as in the case of Fig. 3, they are still similar in many of their details. The oscillations marking the *ab initio* spectra can thus be interpreted as arising primarily from the interference between saddle times. There is no indication of resonance structures in Fig. 3, albeit at these intensities Stark-shift induced resonances are prominent in picosecond pulses [4].

IV. CONCLUSIONS

To conclude, we have shown that for direct (non-recollisional) ionization or detachment of atoms or ions by intense few-cycle pulses, the low-energy part of the angle-integrated energy spectrum can be modulated by an almost periodic succession of peaks and troughs. This modulation can be traced to an energy-dependent interference between the saddle times of the modified classical action. Depending on the duration and peak intensity of the pulse, these peaks and troughs may appear either for carrier-envelope phases close to zero only or for a wider range of phases. They are found in *ab initio* time-dependent calculations as well as in calculations based on the strong field approximation. While much of the calculations presented in this paper are for the case of an helium atom or an He^+ ion exposed to a super-intense pulse, a similar modulation is also observed in atomic hydrogen at intensities as low as $5 \times 10^{13} \text{ W cm}^{-2}$.

Acknowledgments

This work was supported by the A*STAR Computational Resource Centre through the use of its high performance computing facilities. Computers financed by EPSRC have also been used to obtain some of the numerical results presented here. The authors thank B. Piraux for having provided programs the calculation of the *ab initio* results presented here was based on.

Appendix

Here we comment on the key numerical issue in the calculation of the ionization probability within the approach adopted in this work, which is the evaluation of the integral of $\exp[iS(\mathbf{p}, t)]$ over time. As is mentioned in Section II, the usual way of dealing with this integral is to reduce Eq. (15) to Eq. (17). However, a direct numerical intergration, not relying on this approximation, can also be contemplated. Special quadradure methods have then to be used, at least for intense pulses, due to the highly oscillatory nature of the integrand. Classical methods such as Gauss quadratures or the Simpson method converge, but at the cost of a large number of sampling points, which makes them time consuming and inefficient.

We have experimented with a direct integration method based on an approach proposed by Levin [23] and further developed by Evans and Webster [24]. Levin's idea is to make the ansatz

$$\int f(x) \exp[iq(x)] dx = y(x) \exp[iq(x)] \quad (\text{A.1})$$

and, given the functions $f(x)$ and $q(x)$, obtain a differential equation for the unknown function $y(x)$. Levin showed that the relevant solution of this equation can be calculated by a collocation method using a polynomial basis (the choice of the basis eliminates the undesired solutions, which are more oscillatory than the desired solution). However, this method becomes numerically unstable if the number of basis functions is excessively increased in an effort to improve precision. As argued by Evans and Webster [24], using Chebyshev polynomials to form the collocation basis alleviates this problem of numerical stability. Even with this improvement, however, the approach still suffers from another limitation, which is that the systems of coupled linear equations which need to be solved are excessively large for long integration intervals.

We found that this latter limitation can be turned round by subdividing the integration interval into smaller subintervals such that a relatively small Chebyshev basis of 10 to 20 polynomials is sufficient within each subinterval. The subdivision can be automated into an adaptative algorithm which subdivides the intervals until a convergence criteria is met. We noticed that this method is considerably faster than a trapezoidal quadrature of a same degree of accuracy for the intense pulses considered in much of this work.

However, care should be taken that the end point contributions of the integration interval

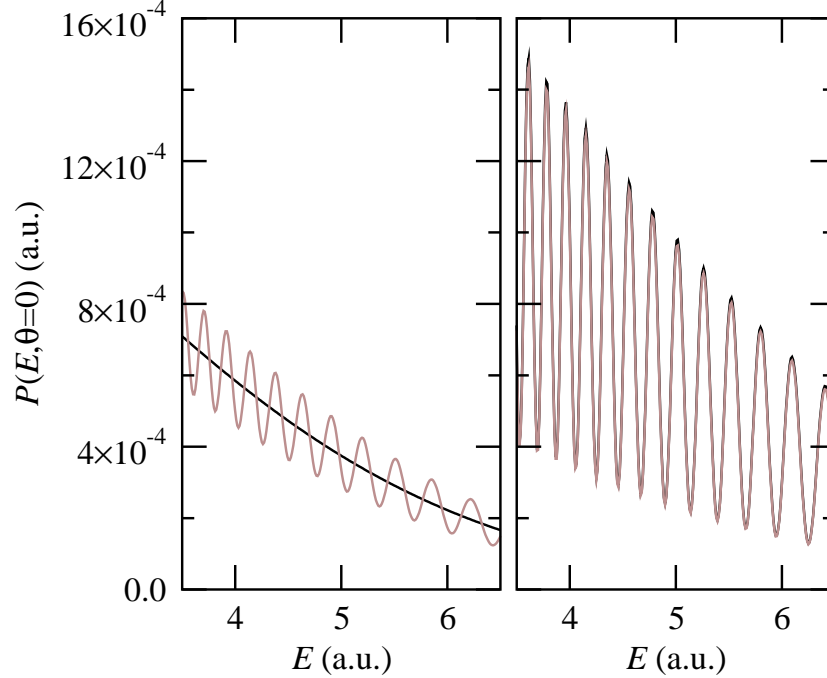


FIG. 8: (Color online) $P(E, \theta)$ at $\theta = 0$ (a) for a 2-cycle pulse, (b) for a 4-cycle pulse. In both (a) and (b) the pulse peak intensity is $5 \times 10^{15} \text{ W cm}^{-2}$, the carrier wavelength is 800 nm, $\varphi = 0$, the amplitude envelope is a \cos^2 function, and the target is He^+ . Light brown curves: results obtained by integrating $\exp[iS(\mathbf{p}, t)]$ along the real axis with the end point contributions removed to first order. Black curves: prediction of Eq. (17).

do not affect the resulting ionization probability (as noted in Section II, these contributions are physically irrelevant). As an example, the ionization probability predicted by Eq. (17) is compared in Fig. 8 to that predicted by Eq. (15) with the integral performed as explained in the previous paragraph. The former decreases monotonically in the case of a 2-cycle pulse, for which only one saddle time (that closest to $t = 0$) contributes significantly, while it oscillates in the case a 4-cycle pulse due to the interference between several saddle times. The small difference between these results and the prediction of Eq. (15) noticeable in panel (b) of the figure is indicative of the accuracy of the saddle point method in this case. However, for the still shorter pulse considered in panel (a), the higher-order contributions of the end points t_i and t_f to the integral of $\exp[iS(\mathbf{p}, t)]$ are not negligible, because in our model the field varies more abruptly at these end points, and these contributions produce spurious oscillations in the ionization probability.

This last difficulty can be avoided by making t complex and deforming the integration

contour into a line running from t_i to $t_i + i\mathcal{C}$ where \mathcal{C} is a positive constant defined below, from $t_i + i\mathcal{C}$ to $t_f + i\mathcal{C}$, and finally from $t_f + i\mathcal{C}$ to t_f . Taking \mathcal{C} equal to the imaginary part of the saddle time closest to the real axis makes the non-end-point contributions of the integrals from t_i to $t_i + i\mathcal{C}$ and from $t_f + i\mathcal{C}$ to t_f negligibly small compared to the integral from $t_i + i\mathcal{C}$ to $t_f + i\mathcal{C}$. Their end-point contributions can be relatively large, but they have no physical meaning and they can be completely removed by integrating only over the line running from $t_i + i\mathcal{C}$ to $t_f + i\mathcal{C}$. Along this line $\exp[iS(\mathbf{p}, t)]$ varies slowly, instead of oscillating rapidly as in the original integral, which makes the numerical quadrature unproblematic.

Finally, we comment on the saddle point approximation, Eq. (17). It could be expected that with increasing intensity, and therefore with increasing values of $S(\mathbf{p}, t)$, saddle integration would become more accurate. However, this is not the case. The reason for this is revealed by examining the cubic term in the Taylor expansion of $S(\mathbf{p}, t)$ about a saddle time. Making the same approximation as that leading to Eq. (21) gives, at a saddle time t_j ,

$$S''(\mathbf{p}, t = t_j) \approx i|E(t_{0j})|\sqrt{2I_p + p_{\perp}^2}, \quad (\text{A.2})$$

$$S'''(\mathbf{p}, t = t_j) \approx |E(t_{0j})|^2. \quad (\text{A.3})$$

Clearly, the term in $S'''(\mathbf{p}, t_j)$ in the Taylor expansion increases with intensity faster than that in $S''(\mathbf{p}, t_j)$, and may therefore become important for strong enough pulses. However, the ordinary saddle time method takes only the latter into account.

Including the cubic term has been considered previously [25]; however, we are not aware that the resulting expression of the ionization amplitude in terms of Airy functions have been used in calculations of the probability of ionization in few-cycle pulses. The saddle point method is easily generalized to include the cubic dependence, though, by making use of the formula

$$\int_{-\infty}^{\infty} \exp\left(-\frac{a}{2}x^2 + i\frac{b}{6}x^3\right) dx = \pi \left(\frac{16}{b}\right)^{1/3} \exp\left(\frac{a^3}{3b^2}\right) \text{Ai}\left[\left(\frac{a^6}{4b^4}\right)^{1/3}\right]. \quad (\text{A.4})$$

Here $a \equiv S''(\mathbf{p}, t_j)/i$ and $b \equiv S'''(\mathbf{p}, t_j)$. Using the asymptotic form of the Airy function Ai [26], this relation reduces in the limit $b \rightarrow 0$ to the familiar equation

$$\int_{-\infty}^{\infty} \exp\left(-\frac{a}{2}x^2\right) dx = \sqrt{\frac{2\pi}{a}}, \quad (\text{A.5})$$

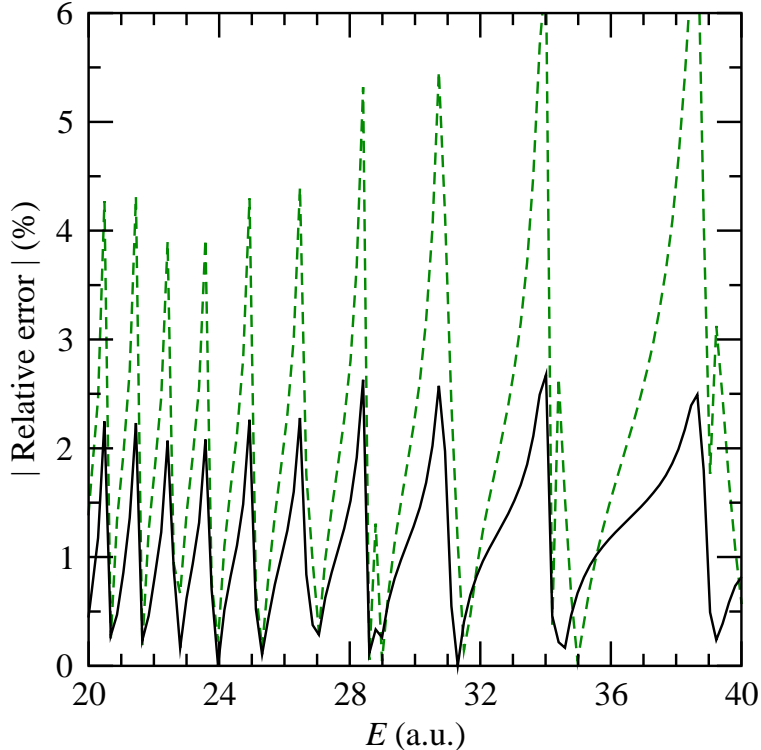


FIG. 9: (Color online) The relative difference between the value of $P(E, \theta)$ calculated by direct integration of $\exp[iS(\mathbf{p}, t)]$ and that calculated by saddle point integration. Dashed curve: the usual saddle point method. Solid curve: the improved saddle point method described in the text. These results refer to the case of an He^+ ion exposed to an 800 nm, 4-cycle \cos^2 pulse of $8.8 \times 10^{15} \text{ W cm}^{-2}$ peak intensity with $\varphi = 0$. Here $\theta = 0$ and the range of energy considered is close to the classical cutoff of $2U_p$ ($2U_p = 38.5 \text{ a.u.}$).

which underpins the ordinary saddle point method. We note with Ortner and Rylyuk [25] that the left-hand side of Eq. (A.4) is formally divergent in applications to the SFA, unless the approximation (A.3) is made, as $S'''(\mathbf{p}, t)$ is normally complex at complex saddle times. Nonetheless, its right-hand side is well defined even for complex values of b . The usual saddle point result of Eq. (17) can thus be improved by replacing the factor of $[2\pi i/S''(\mathbf{p}, t_j)]^{1/2}$ by the right-hand side of Eq. (A.4). In practice, the additional cost is small since fast library routines are available to compute the Airy function of a complex argument.

The improvement in accuracy offered by this method should not be expected to be significant for low peak intensities but can be noticeable for ultra intense pulses. For instance, for the case of a 800 nm pulse of almost $9 \times 10^{15} \text{ W cm}^{-2}$ peak intensity, using Eq. (A.4)

systematically halves the error on the saddle point integration in the higher energy part of the direct ionization spectrum (Fig. 9). The error is also generally reduced in the lower end of the spectrum, although the trend is not as systematic.

-
- [1] P. Agostini, F. Fabre, G. Mainfray, G. Petite, and N. K. Rahman, *Phys. Rev. Lett.* **42**, 1127 (1979).
- [2] W. Becker, F. Grasbon, R. Kopold, D. B. Milosevic, G. G. Paulus, and H. Walther, *Adv. At. Mol. Opt. Phys.* **48**, 35 (2002).
- [3] E.g., G. Petite, P. Agostini, and H. G. Muller, *J. Phys. B* **21**, 4097 (1988).
- [4] R. R. Freeman, P. H. Bucksbaum, H. Milchberg, S. Darack, D. Schumacher, and M. E. Geusic, *Phys. Rev. Lett.* **59**, 1092 (1987).
- [5] G. G. Paulus, W. Nicklich, H. Xu, P. Lambropoulos, and H. Walther, *Phys. Rev. Lett.* **72**, 2851 (1994).
- [6] C. I. Blaga, F. Catoire, P. Colosimo, G. G. Paulus, H. G. Muller, P. Agostini, and L. F. DiMauro, *Nature Phys.* **5**, 335 (2009); F. Catoire, C. I. Blaga, E. Sistrunk, H. G. Muller, P. Agostini, and L. F. DiMauro, *Laser Phys.* **19**, 1574 (2009); W. Quan, Z. Lin, M. Wu, H. Kang, H. Liu, X. Liu, J. Chen, J. Liu, X. T. He, S. G. Chen, H. Xiong, L. Guo, H. Xu, Y. Fu, Y. Cheng, and Z. Z. Xu, *Phys. Rev. Lett.* **103**, 093001 (2009); C. Y. Wu, Y. D. Yang, Y. Q. Liu, Q. H. Gong, M. Wu, X. Liu, X. L. Hao, W. D. Li, X. T. He, and J. Chen, *Phys. Rev. Lett.* **109**, 043001 (2012); H. Liu, Y. Liu, L. Fu, G. Xin, D. Ye, J. Liu, X. T. He, Y. Yang, X. Liu, Y. Deng, C. Wu, and Q. Gong, *Phys. Rev. Lett.* **109**, 093001 (2012).
- [7] See, e.g., C. J. Joachain, N. J. Kylstra and R. M. Potvliege, *Atoms in Intense Laser Fields* (Cambridge University Press, Cambridge, 2012).
- [8] L. V. Keldysh, *Zh. Éksp. Teor. Fiz.* **47**, 1945 (1964) [*Sov. Phys. JETP* **20**, 1307 (1965)].
- [9] G. F. Gribakin and M. Yu. Kuchiev, *Phys. Rev. A* **55**, 3760 (1997).
- [10] C. C. Chirilă and R. M. Potvliege, *Phys. Rev. A* **71**, 021402 (2005).
- [11] A preliminary account of part of the results presented here has been given in C. C. Chirilă, *Analysis of the Strong Field Approximation for Harmonic Generation and Multiphoton Ionisation in Intense Ultrashort Laser Pulses*, PhD Thesis, Durham University (2004).
- [12] If we approximate the corresponding electric field by $-F_0\chi(t)\hat{\epsilon}\cos(\omega t + \varphi)$, thus neglect the

variation of the envelope function $\chi(t)$ when differentiating $\mathbf{A}(t)$, then φ is the phase-angle difference between a peak of the $\cos(\omega t + \varphi)$ carrier wave and the maximum of the electric field envelope.

- [13] See, e.g., M. Dondera, H. G. Muller, and M. Gavrilu, *Laser Phys.* **12**, 415 (2002).
- [14] V. P. Krainov and B. Shokri, *Zh. Éksp. Teor. Fiz.* **107**, 1180 (1995) [*JETP* **80**, 657 (1995)]; V. P. Krainov, *J. Opt. Soc. Am. B* **14**, 425 (1997). See also A. M. Perelomov and V. S. Popov, *Zh. Éksp. Teor. Fiz.* **52**, 514 (1967) [*Sov. Phys. JETP* **25**, 336 (1967)].
- [15] The end-point contributions also vanish in the case of a monochromatic field if $t_f - t_i$ is an integer multiple of the field period and the integral is evaluated for a value of $p^2/2$ satisfying conservation of energy, as in that case $\exp[iS(\mathbf{p}, t)]$ and all its derivatives have the same values at t_i as at t_f .
- [16] A. M. Perelomov, V. S. Popov, and M. V. Terent'ev, *Zh. Éksp. Teor. Fiz.* **51**, 309 (1966) [*Sov. Phys. JETP* **24**, 207 (1967)].
- [17] V. S. Popov, *Usp. Fi. Nauk* **174**, 921 (2004) [*Phys. Usp.* **47**, 855 (2004)].
- [18] As long as the end-point contributions can be neglected and that no allowance is made for the Coulomb interaction at the tunneling stage of the process, the ionization amplitude is also proportional to the integral of $\exp[iS(\mathbf{p}, t)]$ in the Faisal-Reiss (velocity gauge) formulation of the SFA, although with a different overall factor [7].
- [19] N. Bleistein and R. A. Handelsman, *Asymptotic Expansions of Integrals* (Dover, New York, 1986).
- [20] The *ab initio* calculations follow the method described by E. Huens, B. Piraux, A. Bugacov, and M. Gajda, *Phys. Rev. A* **55**, 2132 (1997).
- [21] The argument is of course the same as that leading to the conservation of energy condition $E_N = N\omega - (I_p + U_p)$, where U_p is the ponderomotive energy, for the case of a monochromatic field. Here the comb of peaks is only approximately periodic: the position of the peaks is less and less well predicted by Eq. (23) as E increases.
- [22] Because of the dependence in p_\perp of the right-hand side of Eq. (20), the saddle times have a larger imaginary part for $\theta \approx 90$ deg than for angles closer to 0 or 180 deg. Correspondingly, I_{jk} is suppressed around $\theta = 90$ deg for any pair of saddle times. The regions $\theta \approx 0$ and $\theta \approx 180$ deg also contribute less to the angle integrated spectrum, these ones because of the $\sin \theta$ factor in the angular integral.

- [23] D. Levin, *Math. Comput.* **38**, 531 (1982).
- [24] G. A. Evans and J. R. Webster, *Appl. Numer. Math.* **23**, 205 (1997).
- [25] J. Ortner and V. M. Rylyuk, *J. Phys. B* **34**, 3251 (2001).
- [26] H. A. Antosiewicz, in *Handbook of Mathematical Functions*, edited by M. Abramowitz and I. A. Stegun (U.S. Government Printing Office, Washington, 1972).